1744 *Biochemistry* **2010,** *49,* 1744–1754
DOI: 10.1021/bi901591m

BIOCHEMISTRY
including biophysical chemistry & molecular biology
Article

Regulation of the Ppr Histidine Kinase by Light-Induced Interactions between Its Photoactive Yellow Protein and Bacteriophytochrome Domains

John A. Kyndt,*[,‡] John C. Fitch,[‡] Sven Seibeck,[§] Berthold Borucki,[§] Maarten P. Heyn,[§] Terry E. Meyer,[‡] and Michael A. Cusanovich[‡]

[‡]*Department of Chemistry and Biochemistry, University of Arizona, Tucson, Arizona 85721, and* [§]*Biophysics group, Department of Physics, Freie Universitaet Berlin, Arnimallee 14, 14195 Berlin, Germany*

Received September 10, 2009; Revised Manuscript Received January 22, 2010

ABSTRACT: Ppr is a unique bacteriophytochrome that bleaches rather than forming a far-red-shifted Pfr state upon red light activation. Ppr is also unusual in that it has a blue light photoreceptor domain, PYP, which is N-terminally fused to the bacteriophytochrome domain (Bph). When both photoreceptors are activated by light, the fast phase of Bph recovery (1 min lifetime) corresponds to the formation of an intramolecular long-lived complex between the activated PYP domain and the Bph domain (lifetime of 2−3 days). Since this state is unusually long-lived as compared to other intermediates in the photocycle of both PYP and Bph, we interpret this as formation of a metastable complex between activated PYP and Bph domains that takes days to relax. In the metastable complex, the PYP domain is locked in its activated UV absorbing state and the Bph domain is in a slightly red-shifted state (from 701 to 702 nm), which is photochemically inactive to red or white light. The amount of metastable complex formed increases with the degree of prior activation of PYP, reaching a maximum of 50% when PYP is fully activated compared to 0% when no PYP is activated. The saturation of complex formation at 50% is believed to be due to light-induced heterogeneity within the Ppr dimer. UV irradiation (365 nm) of the metastable complex state photoreverses the activated PYP and the red-shifted Bph to the initial dark state within seconds. We therefore postulate that Ppr functions as a UV−red light sensor and describe the different Ppr states that can be obtained depending on the light quality. Both red and white light upregulate the autokinase activity, while it is downregulated in the dark. The physiological state of Ppr is most likely a mixture of three different states, dark, metastable complex, and red light-activated, with fractional populations whose amounts depend on the light quality of the environment and that regulate the extent of phosphorylation by the kinase.

Ppr is a naturally occurring hybrid of two photoreceptor proteins, photoactive yellow protein (PYP)[1] and bacteriophytochrome (Bph), with a C-terminal histidine kinase (HK) catalytic domain. The gene for this PYP-phytochrome-related (Ppr) protein was discovered in the purple photosynthetic bacterium *Rhodospirillum centenum* (*1*), and more recently in the aerobic anoxygenic phototrophic bacterium *Methylobacterium* 4-46 (Joint Genome Institute). However, it was not until recently that the heterologous production of the fully reconstituted holo-Ppr was reported (*2*). It has been shown that deletion of Ppr in *R. centenum* results in a loss of light regulation of a polyketide synthase gene (PKS), homologous to chalcone synthase genes (CHS) (*1*). An independent study found that PKS regulation is strongly correlated with stress-induced cyst formation in *R. centenum* (*3*). *R. centenum* has an unusual life cycle alternating among free-swimming, swarming, and cyst-forming cells, depending on whether they are grown in liquid or on solid media and the availability of nutrients and light (*4*). Although the enzymatic product of the *R. centenum* PKS has not been determined, in *Azotobacter* species, a PKS synthesizes a special lipid that is part of the cyst outer coat (*5*); thus, a cyst-specific lipid may also be the product of the *R. centenum* PKS. Although an action spectrum is lacking, it is plausible that Ppr is involved in light regulation of cyst formation in *R. centenum*. Moreover, studies with wild-type and Ppr deletion *R. centenum* strains show that there is a change in lipid metabolism upon Ppr deletion (*6*). A gene for the single-domain PYP protein has been found in 18 bacterial species (refs *2*, *7*, and *8* and JGI). Three additional species contain PYP homologues as part of multisensor domain proteins (refs *2* and *9* and JGI), of which only two, Ppr and Ppd, have been heterologously produced and reconstituted (*2*, *9*).

The prototypical single-domain PYP from *Halorhodospira halophila* is a small blue light sensor that has an absorption maximum at 446 nm (*10*). Light excitation initiates a trans−cis

*To whom correspondence should be addressed: Department of Chemistry and Biochemistry, University of Arizona, 1041 E. Lowell St., Tucson, AZ 85721. Telephone: (520) 621-5256. Fax: (520) 621-6603. E-mail: jkyndt@email.arizona.edu.

[1]Abbreviations: apo-holo-Ppr, full-length protein with the biliverdin chromophore only; Bph, bacteriophytochrome; BV, biliverdin; CBD, chromophore binding domain, which comprises the PAS and GAF structural domains of Bph; CHS, chalcone synthase; GAF, acronym formed from cGMP phosphodiesterase, adenyl cyclase, and FhlA proteins which all share this homologous structural motif; Hhal PYP, *H. halophila* PYP; HK, histidine kinase; holo-Ppr, full-length protein containing both chromophores; JGI, Joint Genome Institute; LED, light-emitting diode; PAS, acronym formed from the names of the first three proteins recognized as sharing this sensor motif (periodic clock protein of *Drosophila*, aryl hydrocarbon receptor nuclear translocator of vertebrates, and single-minded protein of *Drosophila*); Pfr, far red light-absorbing form of Bph ($\lambda_{max} \sim 760$ nm); Pnr, blue-shifted form of Bph ($\lambda_{max} \sim 650$ nm); PKS, polyketide synthase; Ppr, PYP-phytochrome related or PYP-Bph-HK; PMSF, phenylmethanesulfonyl fluoride; Pr, red light-absorbing form of Bph ($\lambda_{max} \sim 700$ nm); PYP, photoactive yellow protein.

 Published on Web 01/22/2010

isomerization of the C7−C8 double bond of the chromophore, *p*-hydroxycinnamic acid (pHCA) (*11*, *12*). This is followed by conformational changes in the protein and protonation of the chromophore, which result in several spectrally and temporally distinct intermediates (*10*, *13*). When the chromophore undergoes a trans−cis photoisomerization around its C9 carbonyl, PYP enters the I_1 state which has an absorbance maximum at 465 nm (*14*). In ~120 μs, this intermediate decays to I_2, in which the chromophore ring has moved out toward the solvent and becomes protonated. After ~1.5 ms, PYP undergoes a large conformational change upon formation of the I_2' state, which is associated with the exposure of a hydrophobic surface patch (*10*, *14*, *15*). The protein returns to the initial dark state within ~1 s. I_2' absorbs at ~355 nm and is the longest-lived intermediate, consistent with, but not proving, that it is the signaling state that interacts with a thus far unknown reaction partner. Using Hhal PYP, it has been shown that photoreversal is possible from several intermediates (I_1, I_2, and I_2') in the photocycle, which accelerates the recovery to the dark state up to ~1000-fold (*16*). The same paper also showed, using time-resolved photoreversal measurements, that the I_2 and I_2' states form an equilibrium (designated as an I_2−I_2' equilibrium) and that changes in this equilibrium could provide valuable information about the mechanisms of generating the active state. PYP is considered to be the structural prototype of PAS (Per-ARNT-Sim) signaling domains that are involved in sensing a variety of signals in all domains of life, and these domains have been proposed to have a common mechanism of intramolecular signaling (*18*). The PYP domain from *R. centenum* has all the residues conserved that are thought to be important for chromophore interaction and photoactivation; however, a structural analysis of the isolated domain showed that a residue that is critical for dark reisomerization, M100, adopts a different conformation than in the prototypical Hhal single-domain PYP (*17*), providing an explanation for the ~400-fold slower recovery to the dark state of the PYP domain in Ppr as compared to Hhal PYP (*1*, *2*).

More than 200 Bph homologues have been found to date in a wide variety of bacteria (NCBI Genbank database), and although the vast majority of them appear to occur as a fusion with a C-terminal histidine kinase domain, several variations are found, e.g., fusion with GGDEF (diguanylate cyclase) and EAL (diguanylate phosphodiesterase) domains [*Thermochromatium tepidum* Ppd (*9*)], HK and CheY domains [*Rhodopseudomonas palustris* Bph5 (*2*, *19*)], and methyl-accepting chemotaxis protein signaling domains (*20*, *21*). Almost all of the characterized Bph proteins show a reversible red−far red transition (between Pr and Pfr states) like phytochromes from higher organisms, although there are some exceptions such as *Rh. palustris* Bph3 which forms a reversible blue-shifted Pnr form absorbing at 650 nm (*22*). In most cases, Pr is the dark-adapted state, although this is not universal. The chromophore in Bph that is responsible for photoactivation is biliverdin IXα (BV) (*23*, *24*), and the primary photochemical event that occurs in the Pr to Pfr transition is thought to be isomerization of the C15−C16 double bond between rings C and D of the bilin chromophore (*25*−*27*). Ppr from *R. centenum* has an exceptional Bph in that it does not form a typical far-red form upon illumination (*2*). The dark form, which has a maximum absorbance at 701 nm with a shoulder at 650 nm, becomes bleached when illuminated, resulting in a small residual broad absorption with a maximum around 660 nm. This bleached form has a low extinction coefficient compared to the dark state and does not appear to be photoreversible, which makes it significantly different from the Pnr in Bph3, which has a large extinction coefficient and readily photoreverses. The recovery of the Bph domain to the dark state in Ppr is biphasic after red light illumination and takes several tens of minutes (*28*). However, when the PYP domain also becomes activated (e.g., with white light or blue following red light), the recovery to the dark state becomes triphasic, with an additional faster recovery phase with a duration of ~1 min. This appears to be due to an interaction between activated PYP and Bph, since the fast rate of the recovery of Bph is similar to the PYP recovery rate and such a fast recovery phase is absent in both apo-holo-Ppr (which lacks the PYP chromophore) and recovery after red light illumination (where PYP is not activated) (*28*). A presumed interaction between PYP and Bph domains is also consistent with studies of the isolated PYP domain that show the importance of the C-terminal domain for the PYP photocycle (*29*). On the basis of these observations, it has been proposed that Ppr has, in the course of evolution, exchanged its ability for red−far red photoconversion to a blue−red photoconversion and the function of PYP is to accelerate the recovery of Bph to the dark state (*28*).

Although phytochromes were discovered almost 50 years ago and a large number of homologues have been characterized in plants, algae, fungi, and bacteria (*30*, *31*) (for a recent review, see ref *32*), it was not until recently that crystal structures of bacteriophytochromes became available (*33*, *34*). A structure of the Pr state of the CBD from *Rh. palustris* Bph3, combined with site-directed mutagenesis, demonstrated that the unusual Pr−Pnr transition can be converted into a classical Pr−Pfr transition by a single L207Y mutation (*35*). The residue corresponding to position 207 is conserved as either Y or F in Bph proteins with the classic phenotype; however, it is also conserved as F in Ppr, and therefore not responsible for the unusual bleaching behavior of the Ppr Bph domain. Recently, two structures were reported for the three-domain construct (PAS−GAF−PHY) from *Pseudomonas aeruginosa* (*36*) and *Synechocystis* 6803 Cph1 (*37*), both in their respective dark-state conformations. Both structures reveal that the PHY domain is structurally a member of the PAS family. The PHY domain is connected to the GAF domain with a long helical connector; however, a surprising feature of the PHY domain is a long tonguelike extension that folds back over the GAF domain to seal off the chromophore binding domain. The residues shown to be important for the Pr−Pfr transition in the *P. aeruginosa* structure [Asp194, Ser459, and Arg453 (*36*)] are conserved in Ppr and therefore are not the basis for the lack of Pfr formation in Ppr either. A high-resolution structure of the complete phytochrome molecule including the enzymatic domain is still not available, which leaves the photosensory mechanism in phytochromes unresolved. A recent SAXS study reported the modeling of high-resolution homologous structures into the SAXS data for *Rh. palustris* Bph and thereby revealed for the first time the domain organization in Bph and the relative positions of the chromophores and ATP binding sites in the quaternary structure (*38*).

The discovery of a dual photoreceptor protein like Ppr, with both blue and red light-sensing domains, raises several issues. Does activation of one domain influence the behavior of the other domain (allosteric interactions)? How do the various PAS and GAF domains interact? How are the two input signals integrated? How do the two photoreceptors regulate the kinase domain? We have recently reported that the activated PYP domain appears to accelerate the recovery of

Bph to the dark state (*28*). We now present additional experimental data that show that there are different levels of interaction between PYP and Bph and provide a preliminary model of how these interactions affect the activation of the kinase domain.

MATERIALS AND METHODS

Protein Production. Ppr was heterologously produced in *Escherichia coli* BL21(DE3) using the two-plasmid-based biosynthetic system that was described previously (*28*, *39*). Purification was conducted as described (*28*), the difference being that the cells were resuspended in 50 mM phosphate (pH 7.4), 20% glycerol, and 10 mM NaCl, which was supplemented with 5 mM EDTA, 10 μM leupeptin, and 4 mM PMSF as protease inhibitors. This increased the stability and lifetime of the Ppr, although after 1 week at 4 °C, there were indications of degradation. In some of the preparations, the Calbiochem protease inhibitor cocktail V (100×) was used, with identical results. In addition, the lysate was applied to a Q-Sepharose FF column prior to the TALON column. The sample was loaded on the anion exchange column in 20 mM sodium phosphate (pH 7.4) with 20% glycerol and 10 μM leupeptin (buffer A). A linear gradient was applied using an AKTA Purifier (GE Healthcare) with up to 100% buffer B (buffer A containing 500 mM NaCl). The green-colored Ppr fractions eluted from the Q-Sepharose column with a maximum at ~47% buffer B (~230 mM NaCl). This additional purification step significantly reduced the amount of contaminating isolated PYP domain, which was previously observed to adsorb to the TALON resin. Before the sample was applied to the TALON resin, the phosphate concentration was increased to 50 mM (pH 7.2). The TALON purification was also automated by using the AKTA Purifier with a linear gradient from 0 to 150 mM imidazole. Ppr eluted from the column in 50 mM phosphate, 400 mM NaCl, 20% glycerol, and 90−100 mM imidazole. There was still residual isolated PYP domain that eluted from the TALON column at slightly higher imidazole concentrations. The overlapping fractions that had an increased 435 nm absorbance were not pooled and therefore not used for the described experiments.

UV−Vis Spectroscopy. Absorption spectra and kinetics were recorded using a CARY 300 spectrophotometer. All studies were conducted in 20% glycerol, 50 mM phosphate, 400 mM NaCl, and 100 mM imidazole (pH 7.2), unless otherwise indicated. Although 20% glycerol was found to be necessary for protein stability over several days, there was no significant difference in the reported spectra and kinetics in fresh samples without glycerol. The effect of imidazole was determined in the 10−150 mM range, and no significant spectral or kinetic changes were found. Ppr was bleached by a 40 s exposure to white light (40 W tungsten lamp); subsequent recovery was measured in the dark. Experiments were also conducted with filters to excite only the 701 nm region (red light, Corning K-7, 600 nm cutoff), the 434 nm region (blue light, filter K2+4-72, 460 ± 30 nm), or the near UV region (365 ± 20 nm, filter 7-37). In some experiments, specific LEDs were used to obtain narrow-bandwidth illumination. Absorbance changes were typically measured for up to 300 min at 20 °C, and the kinetic data were fit using Sigmaplot 11 (Systat Software, San Jose, CA). Lifetime is defined as the inverse of the rate constant. To study the longer-lived complex (see below), absorbance was monitored up to 52 h after illumination. In experiments where the effect of phosphorylation on the photobehavior was examined, ATP and $MgCl_2$ were added to final concentrations of 1 and 5 mM, respectively.

Circular Dichroism Spectroscopy. CD spectra were recorded with an upgraded Jasco 500-A spectrometer, as described previously (*40*). The measurement was performed at 10 °C to reduce artifacts from dark reversion during the acquisition of spectra.

Kinase Assay. Ppr fractions that were pooled from the TALON purification were concentrated and washed once with kinase assay buffer [20 mM Tris-HCl (pH 7.8), 100 mM NaCl, and 6 mM $MgCl_2$]. The concentrated Ppr was then diluted ~10-fold to a final concentration of 6 μM in kinase reaction buffer. Six time points were examined for each light condition (1, 3, 6, 12, 20, and 30 min). For each light condition, the sample was preilluminated for 1 min (or kept in the dark for the dark experiment) to produce the desired state, after which ATP was added to a final concentration of 1 mM, which contained ~10% [γ-^{32}P]ATP (~2.5 μCi per reaction; Perkin-Elmer). The sample was kept under continuous illumination during the time course of the experiment (except for the dark-state sample). In the experiment where the metastable complex was examined, the sample was exposed to blue light for 1 min, followed by dark incubation for 400 min, after which the kinase reaction was initiated via addition of ATP. After each time point, the reaction was quenched by mixing with SDS gel loading buffer in a 1:1 ratio. Samples were run on 4 to 20% gels (Precise Hepes gels, Pierce), after which the gel was placed in front of a phosphor storage image screen and incubated for 12 h. The image was digitized using a Typhoon Imager (GE Healthcare), and bands were quantified by volume using ImageQuant TL.

RESULTS

Activated PYP and Bph Domains Form a Metastable Complex. The absorption spectra of purified Ppr, the isolated PYP domain, and apo-holo-Ppr (partially reconstituted Ppr, with only the Bph chromophore present) were published previously (*2*, *28*) and are shown in Figure 1A. The holo-Ppr spectrum appears to be a simple superposition of the spectra of the separate domains, indicating a lack of interaction between the chromophores in the dark state. When illuminated with white light, Ppr shows a bleach of both the PYP absorbance at 435 nm and the Bph absorbance at 701 and 642 nm, with a slight broadening of the Soret (400 nm) absorbance peak (*28*). Illumination with red light only bleaches the Bph absorbance at 701 and 642 nm and leads to broadening of the 400 nm peak due to an absorption change in the tetrapyrrole Soret band. Illumination with blue light alone results in a bleach of the PYP 434 nm absorbance and the formation of an I_2/I_2' intermediate absorbing around 360 nm. Strong blue light will also bleach some of the Bph via the Soret band at 400 nm, which we estimate to be < 1% under the conditions described here (unless otherwise noted). It was previously observed that the recovery of both Bph and PYP, measured at 701 and 435 nm, respectively, is accelerated in white light as compared to the individual blue and red light conditions. The kinetic traces for the recoveries up to 300 min are shown in Figure 2A,B. The corresponding rate constants are summarized in Table 1. These results are very similar to the earlier reported values (compare to Table 1 of ref *28*). However, after blue light and white light illumination, there is a large fraction of the PYP absorbance at 435 nm (~50%) that has not recovered after the two initial recovery phases are completed (see vertical axis and

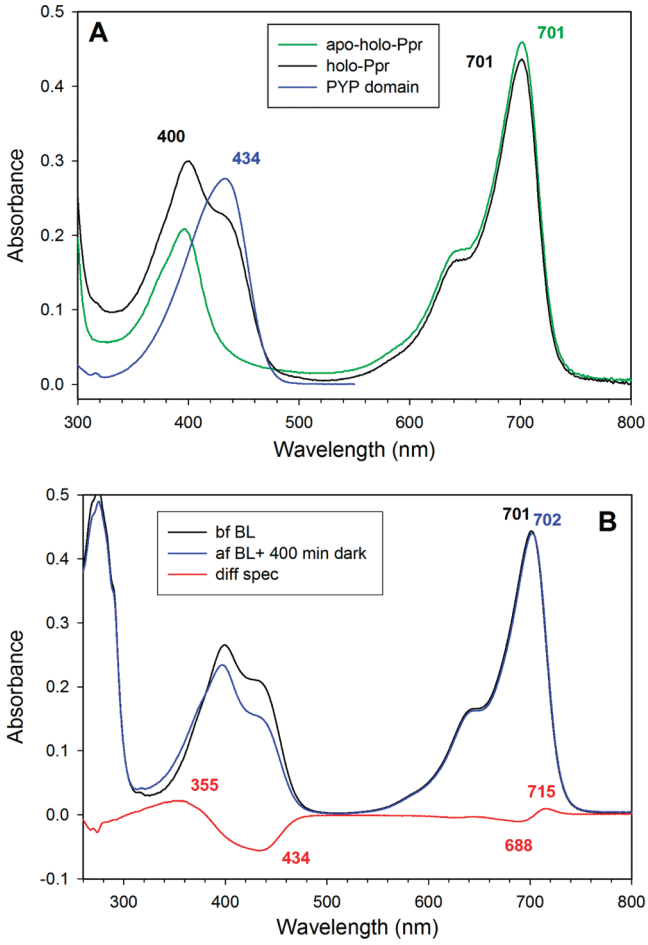

FIGURE 1: (A) UV−vis absorption spectra of dark-state *R. centenum* Ppr (black), the isolated PYP domain (blue), and apo-holo-Ppr (green). Absorbance maxima are indicated for each peak. (B) UV−vis spectra of a Ppr dark-state sample (black), a sample that has recovered for 400 min after blue light activation (blue), and the resulting difference spectrum (red).

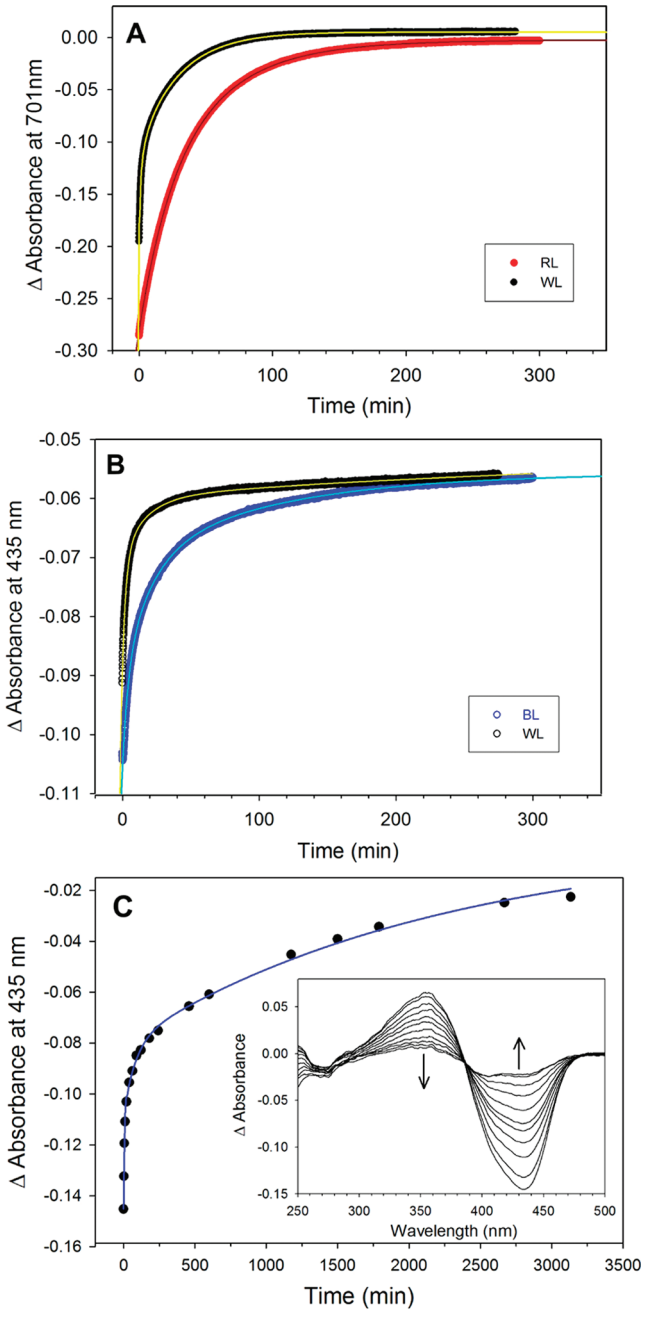

FIGURE 2: Kinetic of recovery of Ppr. (A) Recovery of Ppr after a 40 s white light (black) or red light (red) illumination monitored at 701 nm. (B) Recovery of Ppr after a 40 s white light (black) or blue light (blue) illumination, monitored at 435 nm. All plots were fitted with exponentials, and the resulting rate constants are listed in Table 1. (C) Recovery of 435 nm absorption of Ppr after a 30 s blue light illumination (LED at 470 nm) followed for more than 2 days. The ΔA values at 435 nm are plotted vs time. The inset shows the light minus dark difference spectra in the PYP absorbance region. From the bottom to top at 435 nm: immediately after blue light exposure and after 2, 10, 40, and 121 min and 4, 10, 19.5, 29.5, 44.5, and 52 h in the dark. Arrows indicate the direction of recovery.

end values in Figure 2B). The remainder of the recovery is 1 order of magnitude slower and was monitored over 52 h. The inset of Figure 2C shows the light minus dark difference spectra of Ppr in the PYP spectral domain as a function of time after blue light illumination with an LED emitting at 470 nm. The absorbance values at 433 nm derived from these spectra are plotted in Figure 2C and were fitted with a sum of three exponentials. The fit is colored blue in Figure 2C, and the three corresponding rate constants are given in Table 1. The fit of these longer time data was complicated by the lack of an observed end point (complete return to the baseline was assumed) and possibly some denaturation of the sample; however, it is clear that the third phase has a lifetime of several thousand minutes (2−3 days). We conclude from these results that in addition to the acceleration of recovery previously observed, approximately half of the PYP in the Ppr recovers on an extremely slow time scale after either blue or white light illumination.

The absolute and difference spectra after blue light illumination and 400 min dark recovery (Figure 1B, blue and red traces, respectively) indicate that concomitant with the PYP bleach, there is a small red shift in the 701 nm Bph absorbance, which appears as a minimum at 688 nm and a maximum at 715 nm in the difference spectrum (red trace in Figure 1B). This results in a shift of the observed maximum to 702 nm (blue trace). A very similar difference spectrum was reported earlier for the initial blue light bleach (*28*). The shift at 701 nm was interpreted as an interaction between the activated PYP and dark-state Bph that causes a change in the BV chromophore environment, either through direct interaction at the chromophore binding site or through structural changes propagated over a longer distance through the polypeptide chain (*28*). The data depicted in Figure 1B show that this shift persists together with the PYP bleach for at least 400 min and appears to be kinetically

Table 1: Rate Constants (per minute) and Magnitudes (percentage of total spectral change in italics) for Dark Recovery after White, Red, and Blue Light Excitation of holo-Ppr

λ_{det} (nm)	white	red	blue
701	1.1 (*59*), 0.19 (*9*), 0.03 (*32*)	0.05 (*33*), 0.03 (*67*)	1.6[a]
435	0.20 (*26*), 0.050 (*10*), [0.00028 (*64*)][b]	not available	0.13 (*20*), 0.02 (*21*), [0.00030 (*59*)][b]

[a]Denotes the rate of formation of the 715 nm form. [b]Rate constants in brackets have larger errors because of the instability of Ppr at long times.

associated with the ultraslow recovery of the activated PYP. This state is unusually long-lived compared to other intermediates in the photocycles, and we therefore labeled it as formation of a metastable complex between activated PYP and Bph domains.

In addition to the small red shift in Bph absorbance to 702 nm that occurs in the presence of activated PYP, the maximum bleach of Bph that can be attained under blue and then red light illumination is significantly smaller than that observed without prior blue light activation of PYP (Figure 3A). The maximum steady-state bleach with red light reaches ~75%, and there is a remainder (~25%) of the 701 nm absorbance from unbleached Ppr or, more likely, from a photoproduct absorbing around 650 nm (ref *28* and the red trace in Figure 3A). However, when the sample had been preilluminated with blue light before red light illumination, the maximum steady-state bleach that could be obtained at 701 nm is only ~50% (blue trace in Figure 3A, and see below). This suggests that the metastable complex is no longer photoactive with red light illumination. These results are supported by corresponding CD measurements shown in Figure 3B. The dark CD spectrum (black trace) is typical for the Pr state of bacteriophytochrome with a negative ellipticity around 700 nm, and a positive band in the Soret region (*40*, *41*). Different from a typical bacteriophytochrome is the positive shoulder around 435 nm which is due to the superposition with the weaker positive ellipticity of the PYP chromophore (*42*). Blue light illumination (LED at 470 nm) bleaches the PYP chromophore, leading to a reduced ellipticity around 435 nm (Figure 3B, blue trace). Red light illumination (LED at 680 nm) reduces the ellipticity in the 701 nm region, increases the ellipticity in the 640 nm shoulder, and broadens the Soret region (Figure 3B, red trace). This differs radically from the CD spectra of the Pfr forms of typical bacteriophytochromes in which the ellipticity of the Q-band is close to zero and that of the Soret band is strongly reduced (*43*). However, a very similar pattern of the CD spectrum upon red light illumination was observed with the His250Ala mutant of Agp1 (*44*). If the Ppr sample is first exposed to blue light (5 s, LED at 470 nm), the change in ellipticity induced by red light (5 s, LED at 680 nm) was strongly reduced (Figure 3B, green trace). There are several inferences that can be drawn from these results. The CD data show that the metastable complex that is formed can no longer be bleached, which is consistent with the UV−vis spectral data. Moreover, the observation that the 640 nm increase is only minimal in the blue light preillumination experiment (green trace in Figure 3B) indicates that there is less photoproduct present in this experiment than in the red light experiment (compare the green and red traces in the 640 nm region in Figure 3B).

Figure 3A shows that with blue light preillumination the absorbance decrease at 701 nm with red light is reduced plausibly by the absorbance of the metastable complex formed. By varying the preillumination blue light intensity, we determined the relationship between the extent of Bph bleach with red light

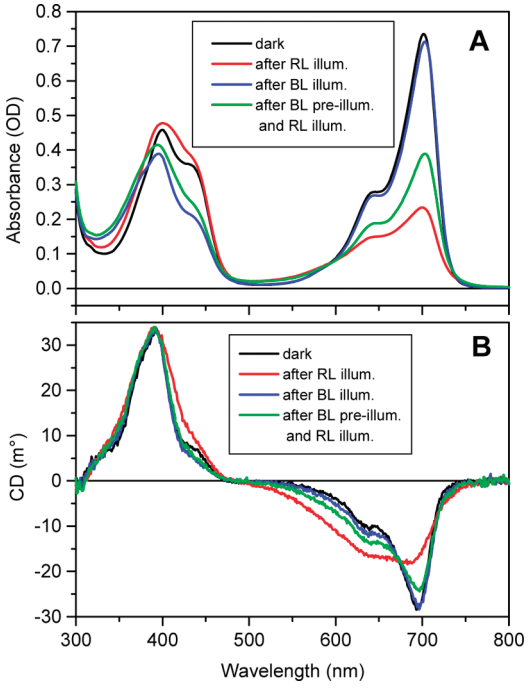

FIGURE 3: Blue preillumination decreases the maximum bleaching of the Bph domain. (A) Effect of red (red trace, 30 s, LED at 680 nm), blue (blue trace, 30 s, LED at 470 nm) and blue preillumination followed by red illumination (green trace) on the absorption spectra of Ppr. The black trace is the dark spectrum. (B) Corresponding effects on the CD spectra. The duration and intensity of the blue light in the two color experiments were the same as in the single-color experiments.

and the amount of previously activated PYP with blue light. The percentage of maximum bleach at 701 nm was found to decrease from ~75% with pure red light illumination to ~50% when PYP was ≥50% activated. This decrease is expected to be due to the formation of a metastable complex. We therefore plotted the residual percentage of the maximum bleach at 701 nm (100 minus the percentage of maximum bleach) as an indirect measurement of the percentage of metastable complex formed, versus the percentage of PYP bleach in Figure 4. This shows that the percentage of metastable complex formed is approximately linear up to ~50% of the maximum PYP bleach under our illumination conditions. That is, when PYP is fully activated with blue light preillumination, only ~50% of the Bph absorption at 701 nm can be bleached. Note that when illuminated with red light alone, there is still ~20−25% residual absorbance at 701 which is assumed to be due to the photoproduct that is formed at 640 nm and a residual fraction of the unbleached dark state (see Figure 3A). In addition, Figure 3B shows that when the sample is preilluminated with blue light prior to red light, there is significantly less photoproduct formed (compare the green and red traces in the 640 nm region). As a consequence, two assumptions were made in plotting the data in Figure 4. We assumed that

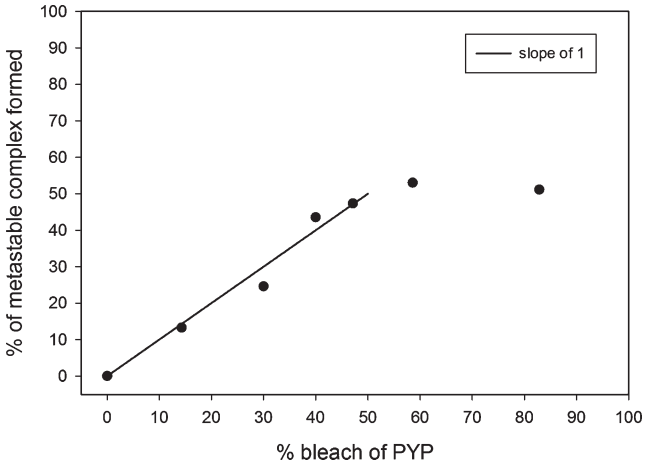

FIGURE 4: Plot of the amount of metastable complex formed [calculated from the bleach of Bph at 701 nm by red light and corrected for the amount of photoproduct (see the text)] that can be achieved after preillumination of the sample with blue light, vs the percentage of the maximum PYP bleach that was obtained with blue light preillumination.

the residual absorbance at 701 nm with red light illumination (~25% of the absorbance) is mainly due to photoproduct absorbance and that this percentage decreases linearly as more metastable complex is formed. When we assume that the percentage due to photoproduct absorbance approaches zero when the sample is illuminated with white light or strong blue light followed by red (full PYP bleach), the curve in the first half of Figure 4 attains a slope of 1, indicating an equimolar interaction between PYP and Bph, up to the 50% saturation point. To obtain the data in Figure 4, we used an equation in which the percent total bleach equals the percentage of observed bleach plus the percentage of photoproduct and made a theoretical calculation for a varying amount of photoproduct (linear correlation from 25 to 0%). The percentage of metastable complex plotted in Figure 4 is then 100 minus the percentage of total bleach. Note that even when this theoretical correction for the varying amount of photoproduct is not made, the percentage of metastable complex formed still saturates at ~50%, however the curve no longer indicates an equimolar interaction. In addition, since PYP absorbance overlaps with the Bph Soret absorbance, the maximum spectral change we could observe at 434 nm is ~60% of the total absorbance at that wavelength, as opposed to 90% of the total absorbance change with the isolated PYP domain. The maximum PYP bleach that could theoretically be obtained is therefore 67% (the ratio 60%/0.90). A similar theoretical maximum for the PYP bleach (~78%) was obtained when the absorbance of apo-holo-Ppr was subtracted from the holo-Ppr spectrum (see spectra in Figure 1A). Since both of these methods have intrinsic errors, the PYP bleach data were normalized in Figure 4 assuming an average theoretical maximum of 70%.

In conclusion, both absorbance and CD measurements suggest that blue light preillumination produces the metastable state which is impaired in the extent to which the Bph can be photoconverted by red light. We will return to this point in the Discussion.

Analysis of the Metastable Complex. To investigate whether the effect of partial recovery of PYP is cumulative, we illuminated with blue light a Ppr sample that had previously been illuminated with blue light and had recovered in the dark for

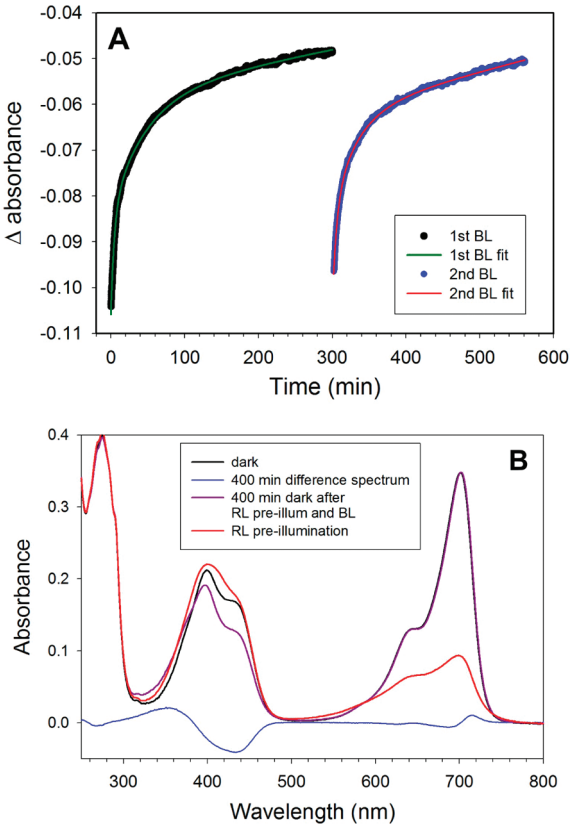

FIGURE 5: (A) Absorbance differences measured at 435 nm after a first blue light bleach of Ppr (black) and after a second blue light bleach after the sample had recovered for 300 min in the dark (blue). The three-exponential fits and corresponding kinetic parameters are colored green and red. Lifetimes for recovery after the first bleach were 5, 46, and ~1500 min and for recovery after the second bleach 5, 32, and ~1200 min. (B) Spectra of Ppr in the dark (black), after red light illumination (red), and after an additional blue light illumination and a 400 min dark recovery (purple). The light minus dark difference spectrum after 400 min is also shown (blue).

300 min (Figure 5A). The second bleach of PYP had less than half the amplitude as compared to the initial blue light PYP bleach, which was to be expected since ~50% of the PYP had not recovered in the 300 min dark recovery. Moreover, after the second blue light bleach, the PYP recovers in 300 min to the same absorbance as prior to the second bleach (Figure 5A), with recovery kinetics similar to the first two phases in Table 1 for the 435 nm recovery. We conclude that all of the PYP capable of forming the metastable complex had done so in the first illumination and that the maximum amount of activated PYP that can form a metastable complex with Bph is thus ~50%. This is consistent with the linear relationship up to ~50% of the maximum PYP bleach, shown in Figure 4.

The results reported here, that is, the partitioning into either metastable state or species capable of recovery to the dark state, could result from a monomer−dimer equilibrium, since phytochrome-containing sensor histidine kinases are typically dimers when functional (*38*, *45*, *46*) but exist in a monomer−dimer equilibrium. To test this possibility, we determined the effect of Ppr concentration [150-fold, from 300 nM to 45 μM (data not shown)] on the kinetics of recovery, since varying the concentration may shift the dimerization equilibrium (depending on the K_D). We found no significant difference in the amount of metastable complex formed as a function of concentration. Thus, it appears that a monomer−dimer equilibrium cannot explain the

two populations of Ppr, one of which forms a metastable complex and one that does not.

To this point, the hypothesis is that metastable complex formation is the result of the interaction of the bleached PYP domain with the dark-state Bph domain. If the interaction were limited to dark-state Bph, one would expect that with red light prebleaching, there would be less dark-state Bph available and therefore less of the PYP would remain unrecovered. To test this hypothesis, the sample was immediately illuminated with blue light after preillumination with red light. On the basis of red light recovery data, we know that the amount of Bph that recovers in the few seconds between the red light and blue light illumination is negligible. The spectra (Figure 5B) and kinetic trace we obtained were essentially the same as in Figures 1 and 2B (e.g., compare the purple trace in Figure 5B to the blue trace in Figure 1B). Thus, preillumination with red light does not have an effect on the amount of PYP that stays unrecovered (~50% of the initial bleach), and activated PYP forms a complex with both activated and dark-state Bph. In addition, since the small red shift in Bph, and therefore the formation of the metastable complex, is observed under both blue light and white light illumination, it appears that its formation is indifferent to the activation of Bph.

We also tested whether phosphorylation of Ppr has an effect on the activated PYP−Bph interaction, that is, whether activated PYP forms a complex with Bph that is stable until Ppr becomes phosphorylated or the extent of complex formation is dependent on the extent of phosphorylation. However, when the sample was illuminated with blue light or white light in the presence of ATP and $MgCl_2$, we found ~50% of the PYP that recovers with a very slow phase (data not shown) and therefore conclude that there is no significant effect of phosphorylation on the amount of metastable complex that is obtained.

To investigate the rate of formation of this metastable complex, we illuminated a dark-state Ppr sample with blue light and monitored the absorbance change at 715 nm. Since blue light does not activate the Bph under these illumination conditions, the only change observed at 715 nm is the formation of the metastable complex (Figure 1B). Because of the small amplitude of the absorbance change at 715 nm, the data are noisy (Figure 6A). However, after the data from three independent measurements were averaged, a rate constant of 1.58 ± 0.31 min^{-1} [lifetime of ~0.63 min (Table 1)] was obtained. Note that this rate is similar to the fast phase of the recovery of Bph after white light illumination in Table 1 (1.1 min^{-1}, lifetime of 0.92 min). The spectrum after a 20 min dark recovery (blue line in Figure 6B) shows indeed that the Bph has shifted its maximum to 702 nm, consistent with formation of the metastable complex.

The Metastable Complex Can Be Photoconverted Back to the Dark State by UV Light. Since it is known that UV excitation of the I_2 and I_2' photocycle intermediates of the homologous single-domain PYP from *H. halophila* results in rapid photoreversal to the dark state (*16*), we investigated whether a similar accelerated recovery of PYP absorbance by UV light occurs in the metastable complex. After Ppr had recovered for 400 min in the dark after blue light illumination, we illuminated the metastable complex with 365 nm (±20 nm) UV light and monitored the spectral changes. As shown in the absorption spectra and difference spectra taken after illumination times with increasing durations (Figure 7A), this resulted in a decrease in absorbance around 355 nm (the I_2−I_2' equilibrium) and an increase around 434 nm (dark state). Interestingly, we observed a simultaneous blue shift from the 702 nm absorbing

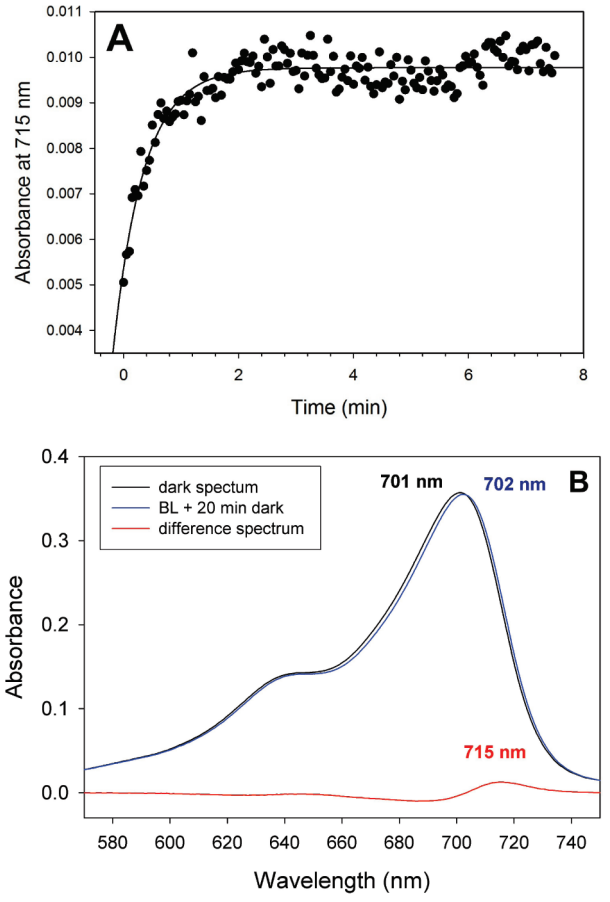

FIGURE 6: (A) Absorbance increase monitored at 715 nm vs time, after blue light illumination of a dark sample. (B) Detail of the UV−vis absorbance of the Bph from Ppr used in panel A. The spectrum for the dark state is colored black; the spectrum for a sample that was blue illuminated, followed by a 20 min dark recovery, is colored blue. The difference spectrum is colored red. Maxima of the absorbance changes are labeled.

Bph back to the dark-state 701 nm form. Figure 7B shows that there is also some bleach in the overall Bph absorbance that is due to unintended excitation of Bph in the Soret band (maximum at ~400 nm) by the UV light. This small portion recovers back to the 701 nm form with kinetics similar to those of the red light-illuminated sample (data not shown). Clearly, the UV illumination converts the metastable complex spectrum to the dark-state spectrum. Although the steady-state photoreversal took several minutes under these illumination conditions, similar results were achieved more efficiently by using an LED emitting at 340 nm. When UV reversal is followed by white light, the kinetics for recovery were identical to those for the initial dark-state Ppr.

Regulation of the Kinase Domain. The autophosphorylation of Ppr was measured under various light conditions. Each experiment was performed by preincubating Ppr in the light for 1 min to obtain the desired photostate similar to the kinetics experiments (or dark for the dark experiments), after which ATP was added. The sample was kept under continuous illumination during phosphorylation (for 30 min) to maintain a photosteady state. Figure 8 shows the radiograms and a plot of the estimated quantifications plotted versus time. It can be seen that both red and white light illumination stimulate autophosphorylation as compared to the sample incubated in the dark, with a net 3−4-fold increase in the extent of phosphorylation. Blue light autophosphorylation measurements were complicated by the fact

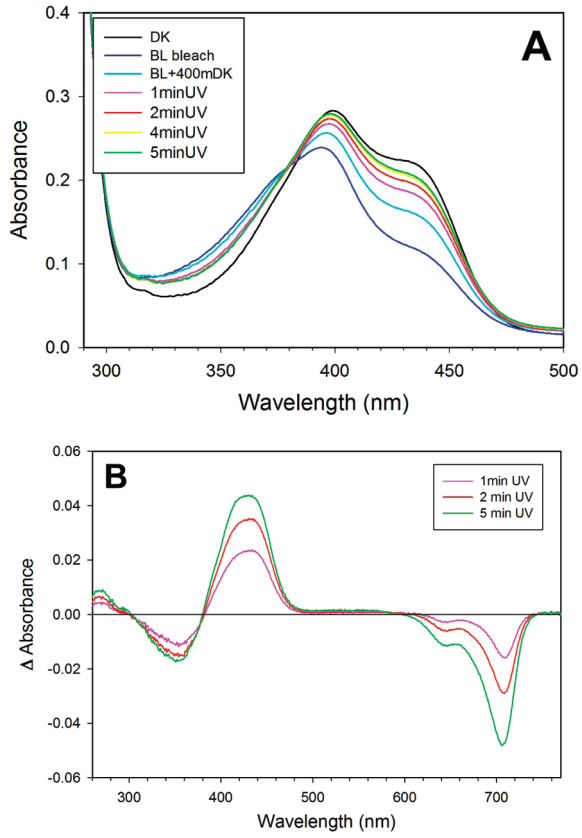

FIGURE 7: UV light-induced spectral changes in Ppr. (A) The black trace is for the dark state (DK). The dark blue trace is a spectrum taken immediately after blue light illumination. The cyan trace is a spectrum of the long-lived state (after a 400 min dark recovery; BL+400mDK). The intermediate spectra are taken after various UV illumination times. (B) Difference spectra from spectra in panel A with respect to the spectrum of the long-lived state (BL+400mDK).

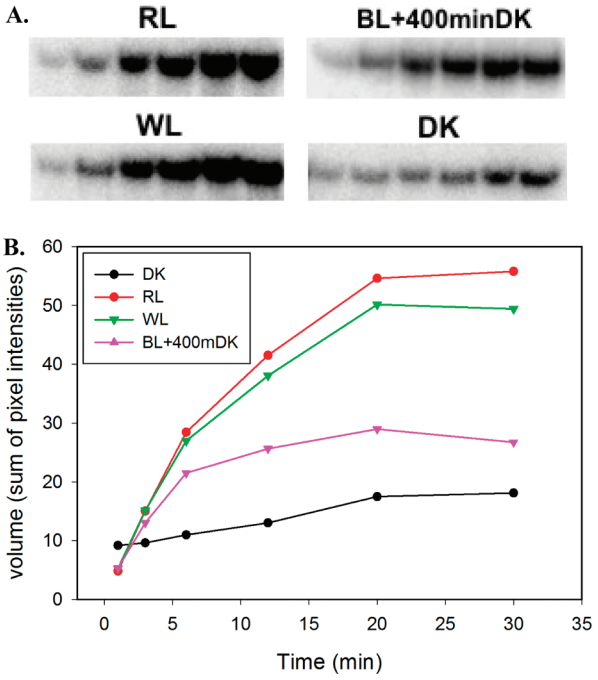

FIGURE 8: (A) Autophosphorylation of Ppr under different light conditions: RL, red light; WL, white light; BL+400 minDK, blue light with a 400 min dark recovery; DK, dark. Individual lanes contained samples taken at different time points (1, 3, 6, 12, 20, and 30 min). (B) Plot of the autophosphorylation intensity (as the sum of pixel intensity) from panel A, with background correction by ImageQuant TL, vs time.

that continuous illumination, even with weak blue light, results in unintended Bph bleach (~30−40%), due to excitation of Bph in its Soret band. The blue light measurements therefore resembled the white light measurements, since both chromophores were excited (data not shown). To determine autophosphorylation with the metastable complex, Ppr was illuminated with blue light, followed by dark recovery for 400 min, after which the autophosphorylation was measured in the dark. Figure 8 shows that the autophosphorylation is activated in the metastable complex, albeit to a lesser extent than under the red or white light conditions.

DISCUSSION

In previous work, we showed that dark recovery of the photoactivated Bph domain in Ppr is accelerated when the PYP domain is simultaneously activated as shown in Figure 2. In this work, we show that when illuminated with blue or white light, approximately half of the activated PYP in Ppr does not recover from the bleached form except on a very slow time scale (irrespective of the state of the Bph domain). Concomitantly, there is a small red shift in the Bph domain absorbance. This red shift, and the fact that following PYP bleaching ~50% of the PYP does not recover to its dark-state spectrum and a similar amount of the Bph is no longer photoactive, is consistent with the formation of a metastable complex containing bleached PYP and the 702 nm Bph form. Clearly, the acceleration of recovery of the Bph absorbance on white light illumination is due to formation of the metastable complex. Complete recovery of Ppr to the dark state takes several days. In the metastable complex, PYP reisomerization is inhibited and the interaction between PYP and Bph results in a spectral perturbation of the bilin chromophore. However, UV light illumination, which photoisomerizes the PYP chromophore back to the trans state, reverses the PYP−Bph interaction, resulting in a small Bph blue shift to the original dark-state spectrum.

Figure 9 summarizes the kinetic observations with red, blue, and white illumination as well as the effects on autophosphorylation. In the dark state, PYP is in its 435 nm absorbing form (shown as PYP blue) and Bph is in the 701 nm form (shown as Bph red), while the kinase is at a low basal level (HK black). With red light illumination, the Bph domain is activated and the kinase is upregulated (HK orange) and the recovery is biphasic, with the two phases having an amplitude ratio of ~2:1 with the slower recovery dominant. The nature of this biphasic recovery is unclear at this point. With both blue and white light, ~50−60% of the Bph domains are rapidly converted to the metastable state, which upregulates the kinase activity (HK orange) and recovers very slowly. In the case of white light illumination, the kinase is fully turned on, similar to the red light situation (all HK orange); however, with blue light illumination, only approximately half of the molecules have the kinase activated. Note that we do not have direct measurement for the kinase activity in the early stages of blue light illumination, and therefore, the HK domains are colored gray. The rest of the blue light-activated PYP molecules recover with biphasic kinetics (with an amplitude ratio of 1:1). The remainder of the bleached Bph domains that do not form the metastable complex after white light illumination recover biphasically, with ~78% having the same rate constant as the slow phase in red light and the other 22% having a rate

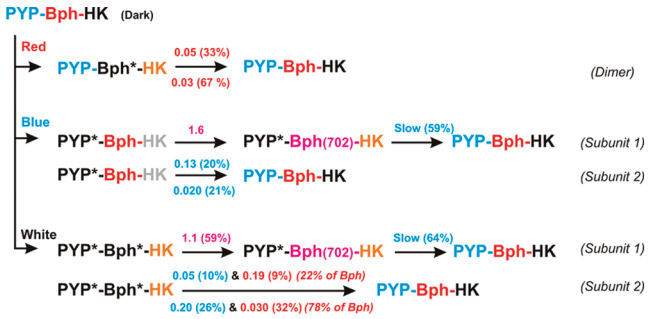

FIGURE 9: Schematic overview of the effects of red, blue, and white light on the Ppr autophosphorylation and recovery kinetics. Dark-state PYP and Bph are colored blue and red, respectively, while activated domains are colored black (with an asterisk). Bph in the metastable complex state is colored pink (with a subscript 702). The HK domain in the dark has a low level of activity and is colored black, while upregulated kinase activity is colored orange. The HK domain colored gray indicates that there is no direct evidence of the kinase activity for that state. Rate constants (inverse minutes) are shown above and below the arrows, and percentages of amplitudes are shown in parentheses. The color of the rate constants corresponds to the recovery of the respective domain (blue for PYP, red for Bph, and pink for formation of the metastable complex).

constant ~4-fold greater than that in red light (0.19 min^{-1} in white light vs 0.05 min^{-1} in red light). This suggests that the formation of the metastable state in one fraction of Bph accelerates the recovery of the Bph domain in the other fraction.

The recovery kinetics of the PYP domain are triphasic in both blue and white light. Approximately 50% forms the metastable state, while the remainder is biphasic. In blue light, the ratio of amplitudes of the two PYP phases which recover relatively rapidly is ~1, with the ratio of rate constants being ~6.5:1. However, in white light, the amplitude ratio of the two PYP phases that recover relatively rapidly is ~2.6:1 and the ratio of their rate constants 4:1, and both rate constants are accelerated relative to those in blue light. This suggests, as seen above, that the formation of the metastable state in one fraction of PYP molecules affects the recovery rate of the other PYP molecules.

Via integration of the spectral and kinetic observations with red, white, and blue light, it appears that ~50% of the dark population can form a metastable complex that traps the PYP domain in a bleached form and the Bph domain in its 702 nm state, which is no longer photoactive. The remaining 50% recovers with two phases, which in aggregate results in ~2-fold acceleration of the Bph domain recovery in white light (weighted contribution of the two 700 nm phases), and a similar acceleration by white light for the PYP domains (weighted average of the two 435 nm phases). Given the complexities of the kinetics and the stability of the Ppr, the overall agreement between the kinetic and spectral data is adequate.

An intriguing aspect of the Ppr mechanism is the fact that the metastable complex formation is limited to ~50% of the molecules. Since we have no direct structural information that could be related to the observed kinetics, we can only speculate about the structural details of the underlying mechanism. However, we found no evidence of a mixture of monomers and dimers in the concentration range used (150-fold). Moreover, gel filtration, dynamic light scattering (data not shown), and preliminary SAXS experiments at millimolar concentrations (M. Papiz, personal communication) show that Ppr is a dimer, similar to other phytochromes. The fact that Figure 4 shows a linear relationship with a slope of 1 between PYP bleach and metastable complex formation indicates that up to ~50% bleaching of PYP by blue light, every activated PYP molecule forms a metastable complex. The activated PYP domains formed beyond the saturation level of 50% do not lead to formation of the metastable complex and recover to dark state with kinetics similar to those of the free domain. Since we currently have no evidence of the existence of two different populations of dimers in our Ppr samples, the simplest hypothesis is that the interaction of the PYP domains with the Bph domains within the Ppr dimer is different between the two monomers and depends on the degree of PYP bleach. This asymmetry could be induced when activation of the PYP domain from one subunit in the dimer prevents stable complex formation in the other subunit, e.g., by blocking access to its PYP−Bph interaction domain, through changing the dark-state subunit structure. Thus, the interactions that occur within the dimer can be described as allosteric, whereby absorption of the first blue photon results in the formation of the metastable state in one subunit and propagates a structural change that prevents formation of the metastable state of the other subunit. This subunit goes through an accelerated photocycle upon absorption of the second blue photon. In essence, we propose that Ppr exists as a blue light-induced heterodimer, with the dark state being a homodimer. Alternatively, the asymmetry could be intrinsic to the dark-state structure. Both possibilities are in agreement with the linear relationship between PYP bleach and metastable complex formation as shown in Figure 4. In this regard, it is interesting to note that tertiary and quaternary plasticity of helices at the dimer interface was observed in the *P. aeruginosa* Bph structure (*36*), which resulted in structural heterodimers. A similar heterogeneity in Ppr could allow for different interactions leading to the heterogeneity in the Ppr recovery kinetics. Asymmetric receptor dimers have also been observed in other nonphotosensing systems, e.g., heterodimers in GPCR systems (*47*, *48*), where receptor homodimer activity can be controlled allosterically by differential ligand binding to each receptor subunit.

The Pr form of most phytochromes converts upon red light illumination to a red-shifted Pfr form. In the case of Ppr, however, no red shift occurs, but instead, the Pr form (701 nm) is bleached, leading to a photoproduct with absorbance centered at ~640 nm. From Figures 3 and 5B, it appears as if only the main 701 band is bleached and the 640 shoulder remains when the bleach is complete. Similar bleached photoproducts with absorption maxima to the blue of the main Q_y band (between 620 and 650 nm) were observed for the Asp197Ala and His250Ala mutants of Agp1 (*49*), and for Agp1 reconstituted with a biliverdin chromophore that had a locked methine bridge between tetrapyrrole rings A and B (*41*). Moreover, the CD spectrum of the Ppr photoproduct shows a striking similarity with that of the His250Ala mutant of Agp1 (*44*). In most phytochromes, the photoconversion proceeds sequentially from Pr via the photointermediates Lumi-R, Meta-R_A, and Meta-R_C to the metastable Pfr form (*50*, *51*). Time-resolved absorption spectroscopy showed that with the Agp1 mutants, the photoconversion was arrested in a Meta-R_A- or Meta-R_C-like intermediate, thus preventing the subsequent Meta-R_C to Pfr transition in which the major red shift occurs (*41*, *49*). For the thermal dark reversion of the Meta-R_A-like photoproduct of Agp1 reconstituted with locked biliverdin, a recovery time of 30 min was observed (*41*), comparable to the recovery times we observed after red light illumination of Ppr (24 and 54 min). These similarities thus suggest that an interaction of the dark PYP domain with the Bph domain leads to a

similar interruption in the photoconversion of Ppr preventing the formation of Pfr. We note, however, that the residues corresponding to Asp197 and His250 of Agp1 are conserved in Ppr. With regard to the nature of the interaction, it is important to mention that during the PYP photocycle there is an exposure of a hydrophobic patch in the bleached UV-absorbing long-lived I_2' state (*10*, *15*, *52*). This "sticky" surface may be involved in the interaction with the Bph domain, although further site-directed mutagenesis and structural analysis will be necessary to identify such an interaction surface. The fact that both PYP and Bph bleach saturate indicates that the interaction is equimolar, at least up to ~50%, and not dependent on the depletion of one over the other. In short, for every mole of activated PYP, 1 mol of Bph goes into the complex, until the 50% limit.

Since the metastable complex state is readily formed and has a long lifetime, it is very likely that this is a physiologically important state of the protein. Once Ppr is in this state, it can function as a red light sensor (there is still up to ~50% bleach with red light), which increases the kinase activity, and it can be reversed to the dark state by UV absorption, where the kinase is downregulated. Since both red and white light upregulate autophosphorylation, we conclude that activation of the Bph domain (either bleached or in the metastable complex) is driving the kinase and that the PYP only serves to control the time course of the upregulation. However, once the protein is in the metastable complex state, blue light does not affect the kinase activity. It is reasonable to speculate that Ppr functions as a UV−red light sensor. One could think of it as a conditional UV−red light switch, where blue light is the condition that activates the switch (through formation of a metastable state). Without the knowledge of the response regulator of Ppr or an action spectrum, it is difficult to speculate about the functional role in the cell. However, it is tempting to explore the possibility that the UV−red light sensing could be consistent with its presumed function in light regulation of cyst formation (*1*, *4*), whereby cyst formation would be repressed under red light conditions where there is sufficient photosynthetic light but activated under higher-intensity UV light which is considered a stress condition. Cells grown under prolonged dark conditions would have the kinase downregulated, although other levels of regulation could also control cyst formation under those conditions. Note that the PKS light regulation reported by Jiang et al. (*1*) was only 2−3-fold, while studies with hyper-cyst mutants have proven that at least 50-fold regulation of PKS levels occurs to control cyst formation, which indicates that multiple regulators are at play (*4*). A few papers have described the possible role of light in bacterial aggregation, mainly during stalk formation of *Stigmatella* (for a review, see ref *53*). In that organism, light is required for the formation of stable mounted aggregates that can produce fruiting bodies when cells are grown on an inorganic salt and agar medium (*54*). A study of the light quality of the photocontrol of this system indicated that the largest response is to light with maxima around 450 nm and to a lesser degree to light of 750 nm (*54*). It is intriguing that *Stigmatella* has two genes for PYP and two genes for phytochromes in the genome (J. Craig Venter Institute, www.jcvi.org), of which the expected absorption maxima could match this action spectrum.

Our novel understanding of the mechanism of Ppr kinase regulation indicates that PYP could function as a UV sensor when complexed with Bph. This sheds new light on the function of PYP and might have similarities in other PYP sensors. The most similar characterized homologue of Ppr is the PYP-phytochrome-diguanylate cyclase Ppd from *Thermochromatium tepidum*. It was shown in the latter that the blue light sensing of the dark state has evolved into a UV-absorbing form (358 nm maximum) and that, at physiological pH, the PYP domain has a photocycle with exclusively UV-absorbing intermediates (*9*). Although the functional role of Ppd is likely to be different from that of Ppr, it appears as if both phytochromes have exchanged their Pr−Pfr reversible transition for a Pr bleaching in which the photocycle is presumably incomplete as compared to traditional Pr−Pfr transitions. Addition of the PYP domain permits UV−red light sensitivity. It remains to be seen if UV sensing is also important for the function of the single-domain PYP systems.

REFERENCES

1. Jiang, Z. Y., Swem, L. R., Rushing, B. G., Devanathan, S., Tollin, G., and Bauer, C. E. (1999) Bacterial photoreceptor with similarity to photoactive yellow protein and plant phytochromes. *Science 285*, 406–409.
2. Kyndt, J. A., Meyer, T. E., and Cusanovich, M. A. (2004) Photoactive yellow protein, bacteriophytochrome, and sensory rhodopsin in purple phototrophic bacteria. *Photochem. Photobiol. Sci. 3*, 519–530.
3. Berleman, J. E., and Bauer, C. E. (2004) Characterization of cyst cell formation in the purple photosynthetic bacterium *Rhodospirillum centenum*. *Microbiology 150*, 383–390.
4. Berleman, J. E., Hasselbring, B. M., and Bauer, C. E. (2004) Hyper-cyst mutants in *Rhodospirillum centenum* identify regulatory loci involved in cyst cell differentiation. *J. Bacteriol. 186*, 5834–5841.
5. Funa, N., Ozawa, H., Hirata, A., and Horinouchi, S. (2006) Phenolic lipid synthesis by type III polyketide synthases is essential for cyst formation in *Azotobacter vinelandii*. *Proc. Natl. Acad. Sci. U.S.A. 103*, 6356–6361.
6. Memmi, S., Ipek, F. M., Bauer, C., Kyndt, J., Meyer, T. E., Vanderstraeten, D., Van Beeumen, J. J., and Devreese, B. (2009) A proteomic study of Ppr-mediated photoresponses in *Rhodospirillum centenum* reveals a role as regulator of polyketide synthesis. Manuscript in preparation.
7. Memmi, S., Kyndt, J., Meyer, T., Devreese, B., Cusanovich, M., and Van Beeumen, J. (2008) Photoactive yellow protein from the halophilic bacterium *Salinibacter ruber*. *Biochemistry 47*, 2014–2024.
8. Kumauchi, M., Hara, M. T., Stalcup, P., Xie, A., and Hoff, W. D. (2008) Identification of six new photoactive yellow proteins: Diversity and structure-function relationships in a bacterial blue light photoreceptor. *Photochem. Photobiol. 84*, 956–969.
9. Kyndt, J. A., Fitch, J. C., Meyer, T. E., and Cusanovich, M. A. (2005) *Thermochromatium tepidum* photoactive yellow protein/bacteriophytochrome/diguanylate cyclase: Characterization of the PYP domain. *Biochemistry 44*, 4755–4764.
10. Meyer, T. E., Yakali, E., Cusanovich, M. A., and Tollin, G. (1987) Properties of a water-soluble, yellow protein isolated from a halophilic phototrophic bacterium that has photochemical activity analogous to sensory rhodopsin. *Biochemistry 26*, 418–423.
11. Kort, R., Vonk, H., Xu, X., Hoff, W. D., Crielaard, W., and Hellingwerf, K. J. (1996) Evidence for *trans-cis* isomerization of the *p*-coumaric acid chromophore as the photochemical basis of the photocycle of photoactive yellow protein. *FEBS Lett. 382*, 73–78.
12. Unno, M., Kumauchi, M., Sasaki, J., Tokunaga, F., and Yamauchi, S. (2000) Evidence for a protonated and *cis* configuration chromophore in the photobleached intermediate of photoactive yellow protein. *J. Am. Chem. Soc. 122*, 4233–4234.
13. Xie, A., Kelemen, L., Hendriks, J., White, B. J., Hellingwerf, K. J., and Hoff, W. D. (2001) Formation of a new buried charge drives a large-amplitude protein quake in photoreceptor activation. *Biochemistry 40*, 1510–1517.
14. Genick, U. K., Soltis, S. M., Kuhn, P., Canestrelli, I. L., and Getzoff, E. D. (1998) Structure at 0.85 Å resolution of an early protein photocycle intermediate. *Nature 392*, 206–209.
15. Borucki, B., Devanathan, S., Otto, H., Cusanovich, M. A., Tollin, G., and Heyn, M. P. (2002) Kinetics of proton uptake and dye binding by photoactive yellow protein in wild type and in the E46Q and E46A mutants. *Biochemistry 41*, 10026–10037.
16. Joshi, C. P., Borucki, B., Otto, H., Meyer, T. E., Cusanovich, M. A., and Heyn, M. P. (2005) Photoreversal kinetics of the I_1 and I_2 intermediates in the photocycle of photoactive yellow protein by double flash experiments with variable time-delay. *Biochemistry 44*, 656–665.

17. Rajagopal, S., and Moffat, K. (2003) Crystal structure of a photoactive yellow protein from a sensor histidine kinase: Conformational variability and signal transduction. *Proc. Natl. Acad. Sci. U.S.A. 100*, 1649–1654.
18. Cusanovich, M. A., and Meyer, T. E. (2003) Photoactive yellow protein: A prototypic PAS domain sensory protein and development of a common signaling mechanism. *Biochemistry 42*, 4759–4770.
19. Larimer, F. W., Chain, P., Hauser, L., Lamerdin, J., Malfatti, S., Do, L., Land, M. L., Pelletier, D. A., Beatty, J. T., Lang, A. S., Tobita, F. R., Gibson, J. L., Hanson, T. E., Bobst, C., Torres, J. L., Peres, C., Harrison, F. H., Gibson, J., and Harwood, C. S. (2004) Complete genome sequence of the metabolically versatile photosynthetic bacterium *Rhodopseudomonas palustris*. *Nat. Biotechnol. 22*, 55–61.
20. Yoshihara, S., and Ikeuchi, M. (2004) Phototactic motility in the unicellular cyanobacterium *Synechocystis* sp. PCC6803. *Photochem. Photobiol. Sci. 3*, 512–518.
21. Yoshihara, S., Katayama, M., Geng, X., and Ikeuchi, M. (2004) Cyanobacterial phytochrome-like PixJ1 holoprotein shows novel reversible photoconversion between blue- and green-absorbing forms. *Plant Cell Physiol. 45*, 1729–1737.
22. Giraud, E., Zappa, S., Vuillet, L., Adriano, J., Hannibal, L., Fardoux, J., Berthomieu, C., Bouyer, P., Pignol, D., and Verméglio, A. (2005) A new type of bacteriophytochrome acts in tandem with a classic bacteriophytochrome to control the antennae synthesis in *Rhodopseudomonas palustris*. *J. Biol. Chem. 280*, 32389–32397.
23. Lamparter, T., Michael, N., Mittmann, F., and Esteban, B. (2002) Phytochrome from *Agrobacterium tumefaciens* has unusual spectral properties and reveals an N-terminal chromophore attachment site. *Proc. Natl. Acad. Sci. U.S.A. 99*, 11628–11633.
24. Bhoo, S. H., Davis, S. J., Walker, J., Karniol, B., and Vierstra, R. D. (2001) Bacteriophytochromes are photochromic histidine kinases using a biliverdin chromophore. *Nature 414*, 776–779.
25. Rudiger, W., Thummler, F., Cmiel, E., and Scheinder, S. (1983) Chromophore structure of the physiologically active form (P(fr)) of phytochrome. *Proc. Natl. Acad. Sci. U.S.A. 80*, 6244–6248.
26. Matysik, J., Hildebrandt, P., Schlamann, W., Braslavsky, S. E., and Schaffner, K. (1995) Fourier-transform resonance Raman spectroscopy of intermediates of the phytochrome photocycle. *Biochemistry 34*, 10497–10507.
27. Andel, F., Lagarias, J. C., and Mathies, R. A. (1996) Resonance raman analysis of chromophore structure in the lumi-R photoproduct of phytochrome. *Biochemistry 35*, 15997–16008.
28. Kyndt, J. A., Fitch, J. C., Meyer, T. E., and Cusanovich, M. A. (2007) The photoactivated PYP domain of *Rhodospirillum centenum* Ppr accelerates recovery of the bacteriophytochrome domain after white light illumination. *Biochemistry 46*, 8256–8262.
29. Kamikubo, H., Koyama, T., Hayashi, M., Shirai, K., Yamazaki, Y., Imamoto, Y., and Kataoka, M. (2008) The photoreaction of the photoactive yellow protein domain in the light sensor histidine kinase Ppr is influenced by the C-terminal domains. *Photochem. Photobiol. 84*, 895–902.
30. Siegelman, H. W., and Firer, E. M. (1964) Purification of phytochrome from oat seedlings. *Biochemistry 3*, 418–423.
31. Butler, W. L., Hendricks, S. B., and Siegelman, H. W. (1964) Action spectra of phytochrome *in vitro*. *Photochem. Photobiol. 3*, 521–528.
32. Rockwell, N. C., Su, Y. S., and Lagarias, J. C. (2006) Phytochrome structure and signaling mechanisms. *Annu. Rev. Plant Biol. 58*, 837–858.
33. Wagner, J. R., Brunzelle, J. S., Forest, K. T., and Vierstra, R. D. (2005) A light-sensing knot revealed by the structure of the chromophore-binding domain of phytochrome. *Nature 438*, 325–331.
34. Wagner, J. R., Zhang, J., Brunzelle, J. S., Vierstra, R. D., and Forest, K. T. (2007) High resolution structure of *Deinococcus* bacteriophytochrome yields new insights into phytochrome architecture and evolution. *J. Biol. Chem. 282*, 12298–12309.
35. Yang, X., Stojkovic, E. A., Kuk, J., and Moffat, K. (2007) Crystal structure of the chromophore binding domain of an unusual bacteriophytochrome, RpBphP3, reveals residues that modulate photoconversion. *Proc. Natl. Acad. Sci. U.S.A. 104*, 12571–12576.
36. Yang, X., Kuk, J., and Moffat, K. (2008) Crystal structure of *Pseudomonas aeruginosa* bacteriophytochrome: Photoconversion and signal transduction. *Proc. Natl. Acad. Sci. U.S.A. 105*, 14715–14720.
37. Essen, L., Mailliet, J., and Hughes, J. (2008) The structure of a complete phytochrome sensory module in the Pr ground state. *Proc. Natl. Acad. Sci. U.S.A. 105*, 14709–14714.
38. Evans, K., Grossmann, J. G., Fordham-Skelton, A. P., and Papiz, M. (2006) Small-angle X-ray scattering reveals the solution structure of a bacteriophytochrome in the catalytically active Pr state. *J. Mol. Biol. 364*, 655–666.
39. Kyndt, J. A., Vanrobaeys, F., Fitch, J. C., Devreese, B. V., Meyer, T. E., Cusanovich, M. A., and Van Beeumen, J. J. (2003) Heterologous production of *Halorhodospira halophila* holo-photoactive yellow protein through tandem expression of the postulated biosynthetic genes. *Biochemistry 42*, 965–970.
40. Borucki, B., Otto, H., Rottwinkel, G., Hughes, J., Heyn, M. P., and Lamparter, T. (2003) Mechanism of Cph1 phytochrome assembly from stopped-flow kinetics and circular dichroism. *Biochemistry 42*, 13684–13697.
41. Seibeck, S., Borucki, B., Otto, H., Inomata, K., Khawn, H., Kinoshita, H., Michael, N., Lamparter, T., and Heyn, M. P. (2007) Locked 5Zs-biliverdin blocks the Meta-R_A to Meta-R_C transition in the functional cycle of bacteriophytochrome Agp1. *FEBS Lett. 581*, 5425–5429.
42. Borucki, B., Otto, H., Meyer, T. E., Cusanovich, M. A., and Heyn, M. P. (2005) Sensitive circular dichroism marker for the chromophore environment of photoactive yellow protein: Assignment of the 307 and 318 nm bands to the $n \rightarrow \pi^*$ transition of the carbonyl. *J. Phys. Chem. B 109*, 629–633.
43. Borucki, B., Seibeck, S., Heyn, M. P., and Lamparter, T. (2009) Characterization of the covalent and noncovalent adducts of Agp1 phytochrome assembled with biliverdin and phycocyanobilin by circular dichroism and flash photolysis. *Biochemistry 48*, 6305–6317.
44. Seibeck, S. (2008) Ph.D. Thesis, FU Berlin, Berlin (http://www.diss.fu-berlin.de/diss/receive/FUDISS_thesis_000000004254).
45. Otto, H., Lamparter, T., Borucki, B., Hughes, J., and Heyn, M. P. (2003) Dimerization and inter-chromophore distance of Cph1 phytochrome from *Synechocystis*, as monitored by fluorescence homo and hetero energy transfer. *Biochemistry 42*, 5885–5895.
46. Strauss, H. M., Schmieder, P., and Hughes, J. (2005) Light-dependent dimerisation in the N-terminal sensory module of cyanobacterial phytochrome 1. *FEBS Lett. 579*, 3970–3974.
47. Zylbergold, P., and Hebert, T. E. (2009) A division of labor: Asymmetric roles for GPCR subunits in receptor dimers. *Nat. Chem. Biol. 5*, 608–609.
48. Han, Y., Moreira, I. S., Urizar, E., Weinstein, H., and Javtich, J. A. (2009) Allosteric communication between protomers of dopamine class A GPCR dimers modulates activation. *Nat. Chem. Biol. 5*, 688–695.
49. Von Stetten, D., Seibeck, S., Michael, N., Scheerer, P., Mroginski, M. A., Murgida, D. H., Krauss, N., Heyn, M. P., Hildebrandt, P., Borucki, B., and Lamparter, T. (2007) Highly conserved residues Asp-197 and His-250 in Agp1 phytochrome control the proton affinity of the chromophore and Pfr formation. *J. Biol. Chem. 282*, 2116–2123.
50. Zhang, C. F., Farrens, D. L., Bjorling, S. C., Song, P. S., and Kliger, D. S. (1992) Time-resolved absorption studies of native etiolated oat phytochrome. *J. Am. Chem. Soc. 114*, 4569–4580.
51. Borucki, B., von Stetten, D., Seibeck, S., Lamparter, T., Michael, N., Mroginski, M. A., Otto, H., Murgida, D. H., Heyn, P. M., and Hildebrandt, P. (2005) Light-induced proton release of phytochrome is coupled to the transient deprotonation of the tetrapyrrole chromophore. *J. Biol. Chem. 280*, 34358–34364.
52. Meyer, T. E., Tollin, G., Hazzard, J. H., and Cusanovich, M. A. (1989) Photoactive yellow protein from the purple phototrophic bacterium, *Ectothiorhodospira halophila*. Quantum yield of photobleaching and effects of temperature, alcohols, glycerol, and sucrose on kinetics of photobleaching and recovery. *Biophys. J. 56*, 559–564.
53. Losick, R., and Shapiro, L. (1984) Microbial Development, Cold Spring Harbor Laboratory Press, Plainview, NY.
54. White, D., Shropshire, W., Jr., and Stephens, K. (1980) Photocontrol of development by *Stigmatella aurantiaca*. *J. Bacteriol. 142*, 1023–1024.